ELSEVIER

Journal of Structural Geology 26 (2004) 1257–1273

JOURNAL OF STRUCTURAL GEOLOGY

www.elsevier.com/locate/jsg

# Vein mineralization at the Damang Gold Mine, Ghana: controls on mineralization

Andrew J. Tunks[a,*], David Selley[a], Jamie R. Rogers[b], Gary Brabham[c]

[a]*CODES-SRC, University of Tasmania GPO Box 252/79, Hobart, Tasmania, Australia 7000*
[b]*Placer Dome Asia Pacific14 Williams St., Kalgoorlie, W.A., Australia 6439*
[c]*Hellman and Schofield Pty Ltd Suite 36/4 Ventnor Ave, West Perth, W.A., Australia 6005*

Received 3 November 2002; received in revised form 20 July 2003; accepted 14 August 2003

**Abstract**

Two distinct styles of Au mineralization occur at the Damang Gold Mine; Palaeoproterozoic sediments of the Tarkwaian Group host both. One style of mineralization is stratabound within quartz–lithic conglomerates of the Banket Series. The second style of mineralization is associated with an extensive low-displacement, fault–fracture mesh that formed in a compressional stress regime late in the deformational history and after the peak metamorphism. Regional deformation within the Tarkwaian involved initial NW–SE directed shortening ($D_1$). A major NNE-trending $F_1$ anticline hosts the Damang orebody. Broadly N–S shortening during $D_2$ resulted in the formation of E–W-trending thrusts with small displacements. The $D_3$ shortening direction was similar to that of $D_1$. Steep $D_1$ faults were reactivated and a new set of low angle thrusts and associated flat-lying extension veins were formed. The bulk of the mineralization observed at Damang is associated with the low displacement $D_3$ fault fracture mesh. The presence of flat-lying extensional veins and the reactivation of some misoriented $D_1$ structures is indicative of periodic episodes of supralithostatic fluid pressures, low differential stress and fault-valve behavior towards the end of the deformation history.


*Keywords:* Fault fracture mesh; Birimian; Tarkwaian; Gold mineralisation; Damang; West Africa

## 1. Introduction

Most of the known significant gold deposits that occur in the SW part of Ghana were mined by small-scale operations prior to modern development of the resources. However, several greenfields discoveries were made in the 1990s reflecting a greater understanding of the geology. This paper documents the structural controls of the Damang Gold Mine at the regional and deposit scale, and discusses the interplay between an understanding of the structural style and the modeling of the deposit for ore reserve calculation purposes.

The basement stratigraphy of SW Ghana comprises metamorphosed sediments and bimodal volcanics of the Palaeoproterozoic Birimian Supergroup, which are intruded by at least two granitic suites (Leube et al., 1990). On a broad scale the Birimian Supergroup of Ghana can be divided into two lithostratigraphic divisions. The 'basins' are extensive areas comprising fine-grained metamorphosed sedimentary rocks including thick turbidite packages, carbonaceous shales and rare cherts (Fig. 1). The 'belts' are a suite of bimodal volcanics that comprise basaltic and andesitic lavas, felsic volcanics and rare rhyolitic and dacitic lavas. These belts occur as fault bounded NE-trending zones, which exceed 100 km in length (Leube et al., 1990; Fig. 1). The Damang Gold Mine is located in the southern part of the Ashanti Belt (Fig. 1). Radiometric dating by Leube et al. (1990), Davis et al. (1994), Oberthur et al. (1998) and Pigois et al. (2003) indicates that the belt volcanics were deposited between 2240 and 2186 Ma and the Birimian sediments deposited 100–60 Ma later into the basins.

Two distinct granitic suites have intruded the Birimian Supergroup. The Cape Coast-type granitoids are dominantly granodiorites and intrude the basins, whereas the Dixcove type granitoids comprise granodiorite to monzonite and syenite and intrude the belts. The Dixcove granitoids have been dated at 2172 ± 1.4 Ma in the Ashanti Belt (Hirdes et al., 1992) and the Cape Coast type between 2104 ± 2 and 2123 ± 3 Ma in the Kumasi Basin (Oberthur et al., 1998).

Rocks of the Tarkwaian Group include conglomerates, sandstones and subordinate shale. They are spatially restricted to the belts where they unconformably overlie volcanic rocks of the Birimian (Davis et al., 1994). Dating

* Corresponding author.
*E-mail address:* Andrew.Tunks@utas.edu.au (A.J. Tunks).

0191-8141/$ - see front matter © 2004 Elsevier Ltd. All rights reserved.
doi:10.1016/j.jsg.2003.11.005

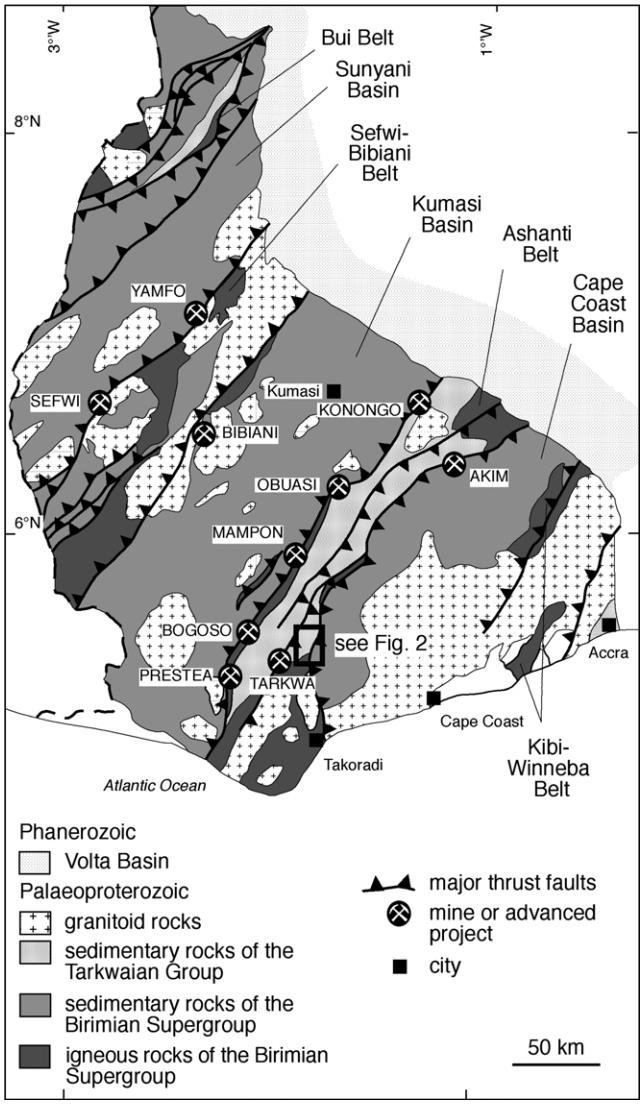


Fig. 1. Regional geology of SW Ghana modified from Allibone et al. (2002a). Area of Damang Mine defined by rectangle. Major gold deposits include Obuasi, Bibiani, Konongo, Bogusu, Prestea and Tarkwa. Several advanced projects are also shown: Akim, Mampon and Yampho Sefwi. Four of the six Birimian volcanic belts are shown, the remainder occur in northern Ghana.

completed by Davis et al. (1994) and more recent work by Pigois et al. (2003) has constrained the maximum age of sedimentation of the Tarkwaian to 2133 ± 4 Ma. Much of the clastic material in the Tarkwaian sediments is derived from the adjacent Birimian units. The relationship between the Tarkwaian Group and the underlying Birimian Volcanics is not well understood due to poor exposure of the contact. Based on similar styles and orientations of deformational fabrics within the Tarkwaian and the Birimian, Eisenlohr and Hirdes (1992) and Hirdes et al. (1992) suggest that the Tarkwaian Group sediments were deposited as a molasse onto actively deforming Birimian basement. Where the Birimian–Tarkwaian contact has been observed in drilling near the Damang mine it is either a faulted contact or an angular unconformity.

Two major orogenic events have been identified. The Eburnian I orogeny (2200–2150 Ma) was associated with the eruption of the Birimian mafic volcanics and intrusion of the Dixcove Granitoids (Allibone et al., 2002b). The Eburnian II orogeny resulted in the strong NE-trending structural grain associated with tight to isoclinal folding of the Birimian sedimentary rocks and major thrust faults, which typically separate the Birimian meta-sediments from the Birimian volcanic belts (Leube et al., 1990; Eisenlohr and Hirdes, 1992; Oberthur et al., 1998). Metamorphic grades within the Birimian meta-sediments and volcanic belts are typically mid to upper-greenschist facies, although amphibolite facies assemblages have been documented in the contact aureoles around the granitoids and more extensively in the southern part of the Ashanti Belt (John et al., 1999). Metamorphic grades within the Tarkwaian are not well documented but appear to range from lower greenschist facies in the area of the Tarkwa Mine up to amphibolite facies in the Damang area to the east of the Damang Fault.

Historically, two distinct styles of Au mineralization have been recognized and mined in Ghana. The first style of Au mineralization occurs solely within quartz lithic and oligomictic conglomerates of the Banket Series within the Tarkwaian Group. The auriferous horizons are perfectly conformable with the hosting strata and economic gold grades are restricted to a few conglomeratic horizons, locally termed 'Banket Reefs' (Blenkinsop et al., 1994). Sestini (1973) and Hirdes and Nunoo (1994) interpret the geological evidence to indicate that the Banket conglomerate hosted gold mineralization within the Tarkwaian is of a paleoplacer origin. The second style of mineralization is gold associated with graphitic–mylonitic shear zones with quartz ± carbonate veins in deformed rocks of the Birimian Supergroup. This mesothermal style is typically associated with extensive arsenopyrite alteration of the host rocks and examples include the plus 30 million ounce Obuasi deposit (Brabham, 1998; Allibone et al., 2002a), the plus six million ounces at Prestea (Appiah, 1991) and the plus 2 million ounce Bogusu Deposits (Allibone et al., 2002b; Fig. 1).

### 1.1. Methods

Detailed geological mapping was carried out within the Damang Gold Mine during ongoing mining. Regional mapping extended south from the Damang Gold Mine to target the prospective Banket Series conglomerates southwards along both limbs of the Damang Anticline (Fig. 2). As is typical in heavily forested tropical areas exposure is not good, but reasonable access was achieved by mapping old adits and over 50 exploration trenches. Field data were supplemented with detailed aeromagnetics acquired on a 40 m line spacing with flying heights of 10–20 m dependent on topography and vegetation. No detailed mapping was carried out within the Birimian volcanics that occur in the core of the Damang Anticline (Fig. 2).

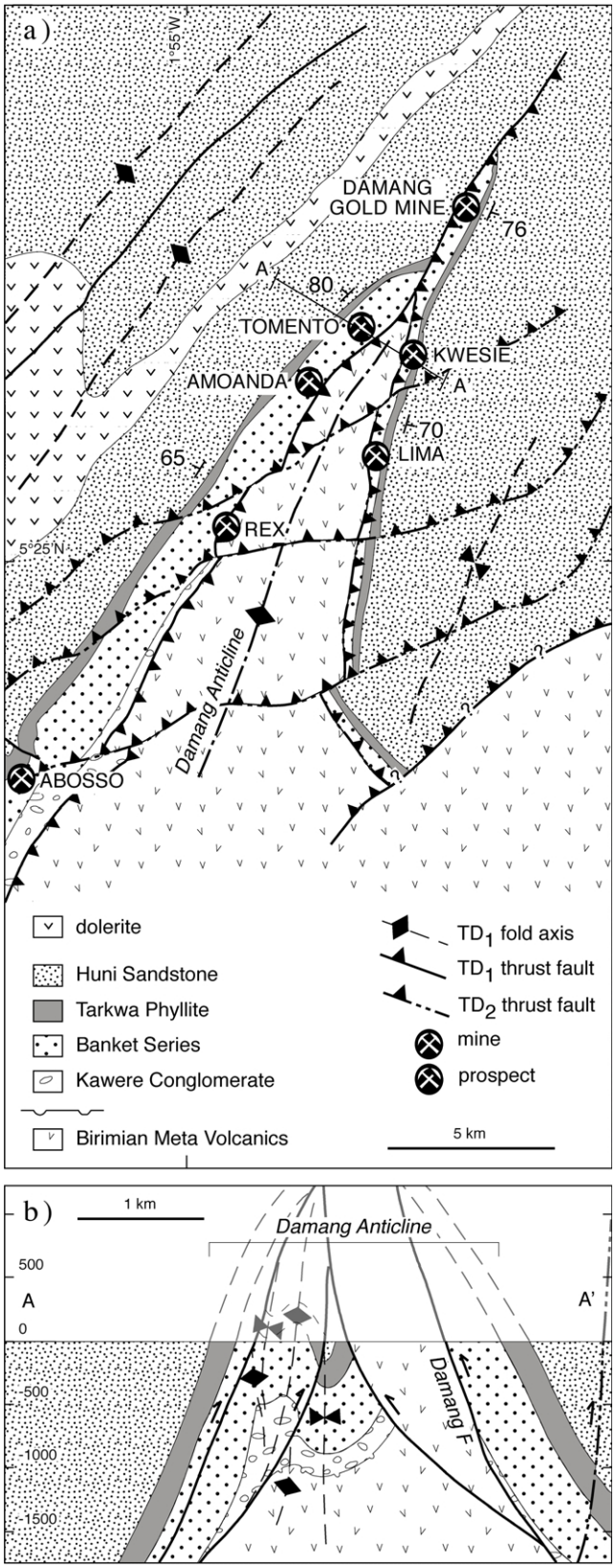


Fig. 2. (a) Regional geology of the Damang Area illustrating the broad scale geometry of the Damang Anticline, the location of the Damang Gold Mine and several other prospects. The Abosso Mine has underground development on high-grade portions of the Banket conglomerate. It was closed for economic reasons in the 1980s. (b) Cross-section demonstrating complexity of the Damang Anticline and internal dismemberment by $TD_1$ thrusts.

## 2. Regional stratigraphy

The Damang region contains Tarkwaian Group metasediments and Birimian volcanic units, with the latter occupying the core of the Damang anticline (Fig. 2). Local stratigraphic subdivisions of the Tarkwaian System have been described by Whitelaw (1929), Hirst (1938), Junner et al. (1942) and Brabham (1998). The detailed stratigraphy of the Tarkwaian Group and its relationship to the underlying Birimian Volcanics is shown in Fig. 3.

The poorly exposed Kawere Group unconformably overlies or is in faulted contact Birimian Volcanics along the western limb of the Damang anticline. The thickness of the group gradually decreases northwards from the Abosso mine site and appears to thin dramatically near the Rex prospect (Fig. 2). The Banket Series can be subdivided into two main lithofacies; quartz–lithic sandstone and the economically important conglomerates which occur near the top of the Banket Series. The predominant clast types within the conglomerates are vein quartz and quartzite with minor fine-grained Birimian volcanics and chert. Matrices of conglomerates are enriched in heavy minerals such as hematite, magnetite, ilmenite, rutile, zircon and gold (Strogen, 1988; Marston et al., 1992).

The Tarkwa Phyllite is a sequence of finely-laminated to thinly-bedded siltstone and mudstone with minor fine-grained sandstone. It is a true phyllite to the west of the Damang Fault and is characterized by a fine-grained, sericite quartz assemblage. However, to the east of the Damang Fault, where it is exposed in the Damang Mine the Tarkwa Phyllite is a foliated garnet–biotite–plagioclase ± staurolite ± epidote ± kyanite ± cordierite rock indicative of amphibolite metamorphic conditions (Pigois et al., 2003).

The youngest Tarkwaian unit preserved in the southern Ashanti Belt is the Huni Sandstone. It comprises a monotonous and poorly preserved sequence of fine- to medium-grained quartz, feldspathic and chloritic sandstone.

In the Tarkwa and Damang regions, mafic sills and dykes comprise up to 20% of the total Tarkwaian stratigraphic section (Junner et al., 1942). The main lithologies observed include metamorphosed dolerite, gabbro, microdiorite and tonalite. Most mafic bodies are semi-conformable with the strike and dip of enclosing strata and their emplacement predates regional folding of Tarkwaian stratigraphy (Brabham, 1998).

## 3. Regional structure

Four phases of compressional deformation are recorded regionally within the Tarkwaian sequence ($TD_1$–$TD_4$). Collectively, these events involve progressive brittle–ductile modification of, or in some cases pronounced dismemberment of, macroscopic upright folds generated at the onset of deformation. Structures and fabrics related to

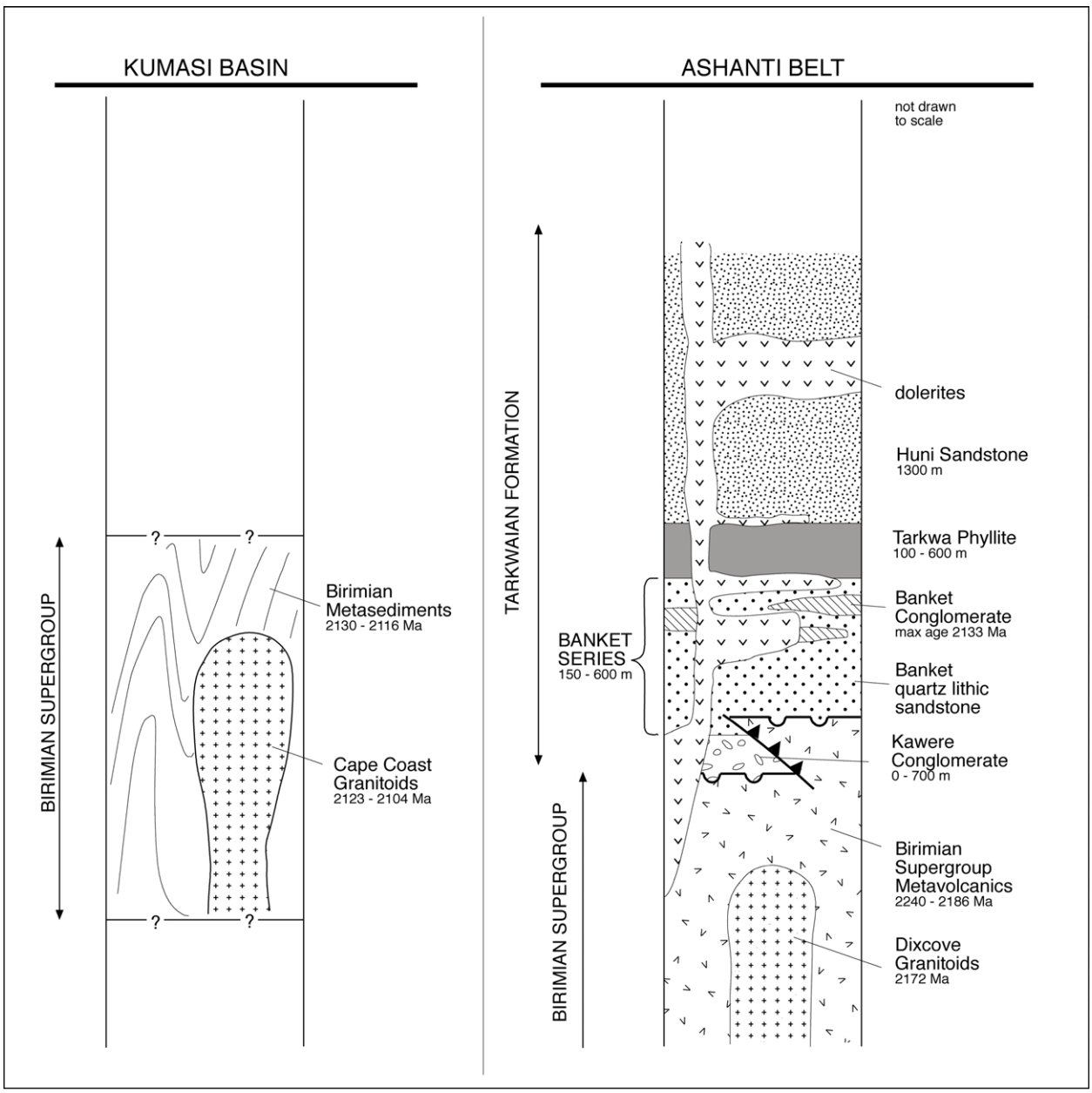


Fig. 3. Regional stratigraphy of the Kumasi Basin and the Ashanti Belt (Southern Region). Age dating provided for units where available (Hirdes et al., 1992; Davis et al., 1994; Oberthur et al., 1998; Allibone et al., 2002b; Pigois et al., 2003).

$TD_1$ and $TD_3$ are most conspicuous, and have the greatest influence on the distribution of known gold mineralization.

Below we summarize the geometric aspects of each deformation phase. The bulk of the data was collected from weathered road cuttings and exposures created from small-scale mining and exploration activities in four principal prospect areas: Rex, Tomento, Lima and Amoanda (Fig. 2).

### *3.1. $TD_1$*

$TD_1$ produced the major macroscopic structures in the Damang region under NW–SE shortening and provided the structural template upon which later deformations were imposed. Major structures include upright, open to close, shallowly NNE–NE plunging folds ($TF_1$) with wavelengths of 1–5 km (Fig. 2).

$TF_1$ closures are commonly non-cylindrical, a geometric response to dismemberment by axial plane sub-parallel thrusts. Non-cylindrical geometries are demonstrated by the distribution of poles to regional bedding data, which plot about a crudely defined SW dipping girdle, but spread close to the primitive circle (Fig. 4a). A more accurate estimation of the initial $TF_1$ geometry comes from a subset of this data at Tomento, where a macroscopic anticline–syncline pair remains largely unmodified (Fig. 5). In this case, poles to bedding show a relatively tight distribution about a

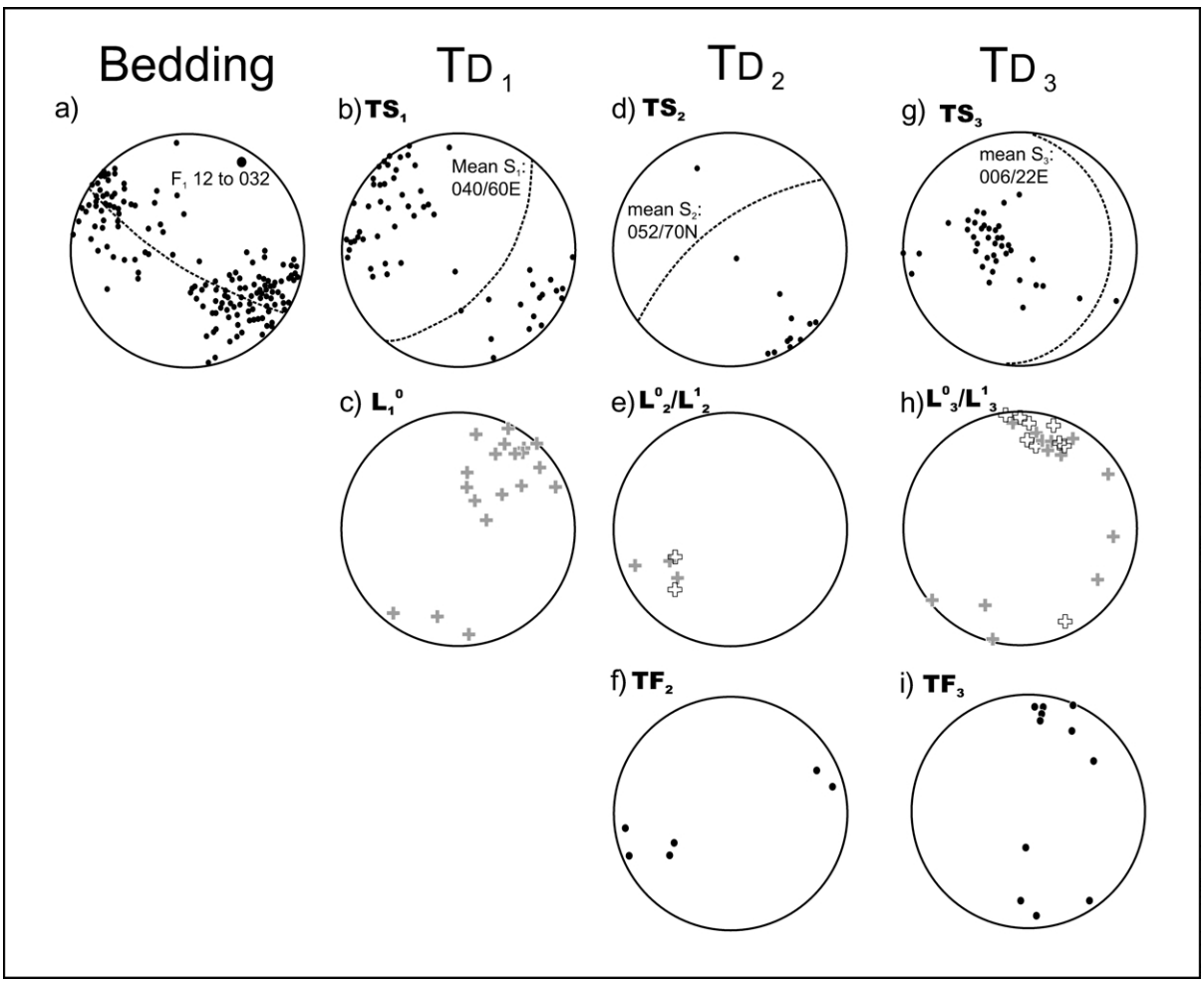


Fig. 4. Lower hemisphere equal area stereonets for regional structural data. (a) Poles to bedding, (b) poles to $S_1$, (c) $L_1^0$ intersection lineations, (d) poles to $S_2$, (e) $L_2^0$ (solid crosses) and $L_2^1$ lineations, (f) measured $TF_2$ fold axes, (g) poles to $S_3$, (h) $L_3^0$ (solid crosses) and $L_3^1$ intersection lineations, (i) measured $TF_3$ fold axes.

shallowly NE plunging rotation axis. This hinge orientation is consistent with the regional NE strike of the $TS_1$ cleavage (variable dip is due in part to refraction), as well as regional $L_1^0$ data (Fig. 3b and c).

NNE–NE striking fault surfaces are developed within the hinges or less commonly limbs of all major $TF_1$ closures. The Damang Fault is the most regionally significant of these structures (Fig. 2a and b). Juxtaposition of different levels of stratigraphy across dismembered hinges at Damang and Rex indicate a significant component of SW-side up reverse displacement (Figs. 2 and 5), whereas SE-verging thrusts occur at Tomento (Fig. 4). We interpret these early faults as 'break-through' thrusts, having accommodated progressive fold tightening during the latter stages of the $TD_1$ event.

### 3.2. $TD_2$

Macroscopic $TD_2$ structures include ENE-striking thrust faults in the vicinity of Rex and immediately south of Abosso (Fig. 2). Bedding in these regions is rotated clockwise of the regional NE structural grain, and minor shallowly WSW–ENE plunging $TF_2$ closures occur with upright to steeply NNE dipping axial surfaces and weak axial planar cleavage development. The geometry of $TD_2$ structures, along with rare ENE striking fault surfaces with down-dip slickenfiber lineations is consistent with their development during a phase of NNW–SSE directed shortening.

### 3.3. $TD_3$

$TD_3$ is characterized by the development of low amplitude folds and spatially associated brittle fracture networks. $TF_3$ fold wavelengths are generally less than 5 m, with gentle to open, asymmetric profiles and characteristically shallowly dipping axial surfaces. Despite the low strains associated with folding, the $TS_3$ cleavage is the most pervasively developed planar fabric observed in many field exposures, occurring as a spaced crenulation cleavage in Tarkwa Phyllite and as a spaced fracture cleavage in coarser-grained lithotypes. The shallow mean dip of $TS_3$ (006/22°E) is shown in Fig. 4g with correspondingly shallow plunges of $TF_3$ hinge lines, $L_3^0$ and $L_3^1$ lineations,

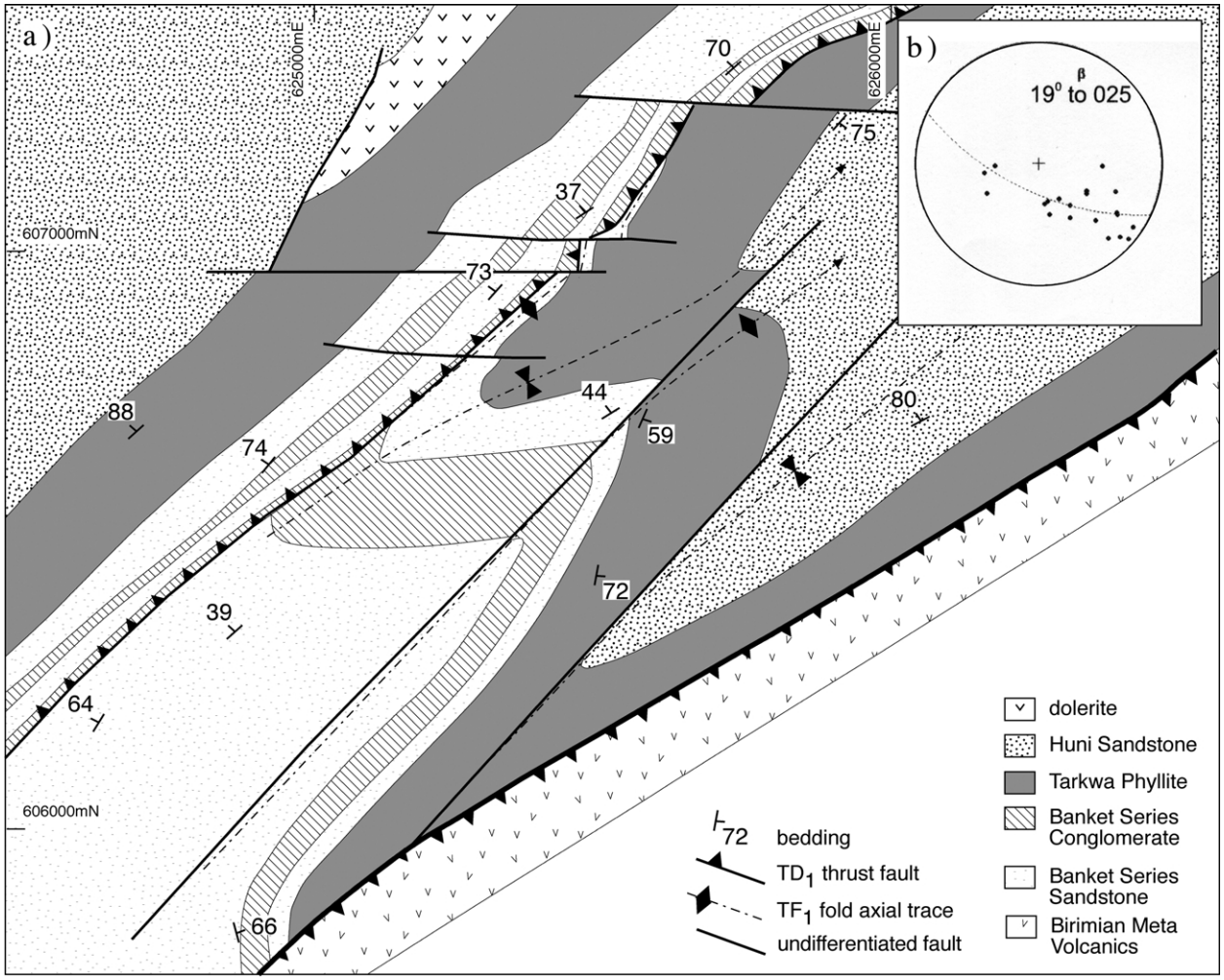


Fig. 5. (a) Detailed geology of the Tomento region. Prospective Banket Series stratigraphy is folded about NE–NNE plunging, upright $TF_1$ closures. Thrust surfaces with SE transport dismember macroscopic $TF_1$ anticline in NW of prospect. (b) Lower hemisphere equal area stereographic projection of poles to bedding: calculated $\beta$-axis approximates $TF_1$ hinge.

each displaying dominant NNE–SSW trends. The orientation of $TF_3$ and associated linear elements indicates ESE–WNW directed shortening during $TD_3$, slightly anticlockwise to that interpreted for $TD_1$.

$TD_3$ brittle fracture networks involve a complex association of moderately to shallowly dipping thrusts, less common steeply dipping faults with variable strike-slip components, and quartz veins. Fault gouges are typically darker and finer grained than their immediate wall rocks, a feature related to cataclastic grain-size reduction. Internally, they possess a variety of textures including crackle breccia and mesoscopically ductile fabrics such as shear bands, rootless folds and shear foliation. Thicknesses of fault gouges range from individual sub-millimeter seams, commonly oriented sub-parallel to bedding, to a maximum of 1.5 m. Displacements along the broadest of these structures are poorly constrained, although measurable offsets associated with faults up to 30 cm in thickness are in the order of a few centimeters at most.

At least two generations of quartz veins were developed regionally during $TD_3$. The earliest generation possesses a variety of orientations, but most commonly form arrays of stacked, flat-lying to moderately dipping veins. Individual veins range from 0.1 to 50 cm in thickness and display subplanar to crudely lensoidal form. A spatial association with brittle $TD_3$ faults is ubiquitous, and they are typically developed as tensional veins arrays concentrated about minor thrust faults. Although veins may be offset by thrust faults (rarely more than a centimeter or so), frequent mutually cross-cutting relationships between both structural elements indicate broadly contemporaneous development. Selvages to many early $TD_3$ veins and associated brittle faults are pyritic and gold-bearing. The later vein generations are typically pyrite-poor, and although oriented similarly to early generations, are more laterally extensive, planar, and cross-cut brittle fault zones without offset.

Lack of evidence for considerable displacement associated with $TD_3$ faults is in accordance with the minor shortening accommodated by $TF_3$ folds. Structures of this generation are interpreted to have limited along-strike and

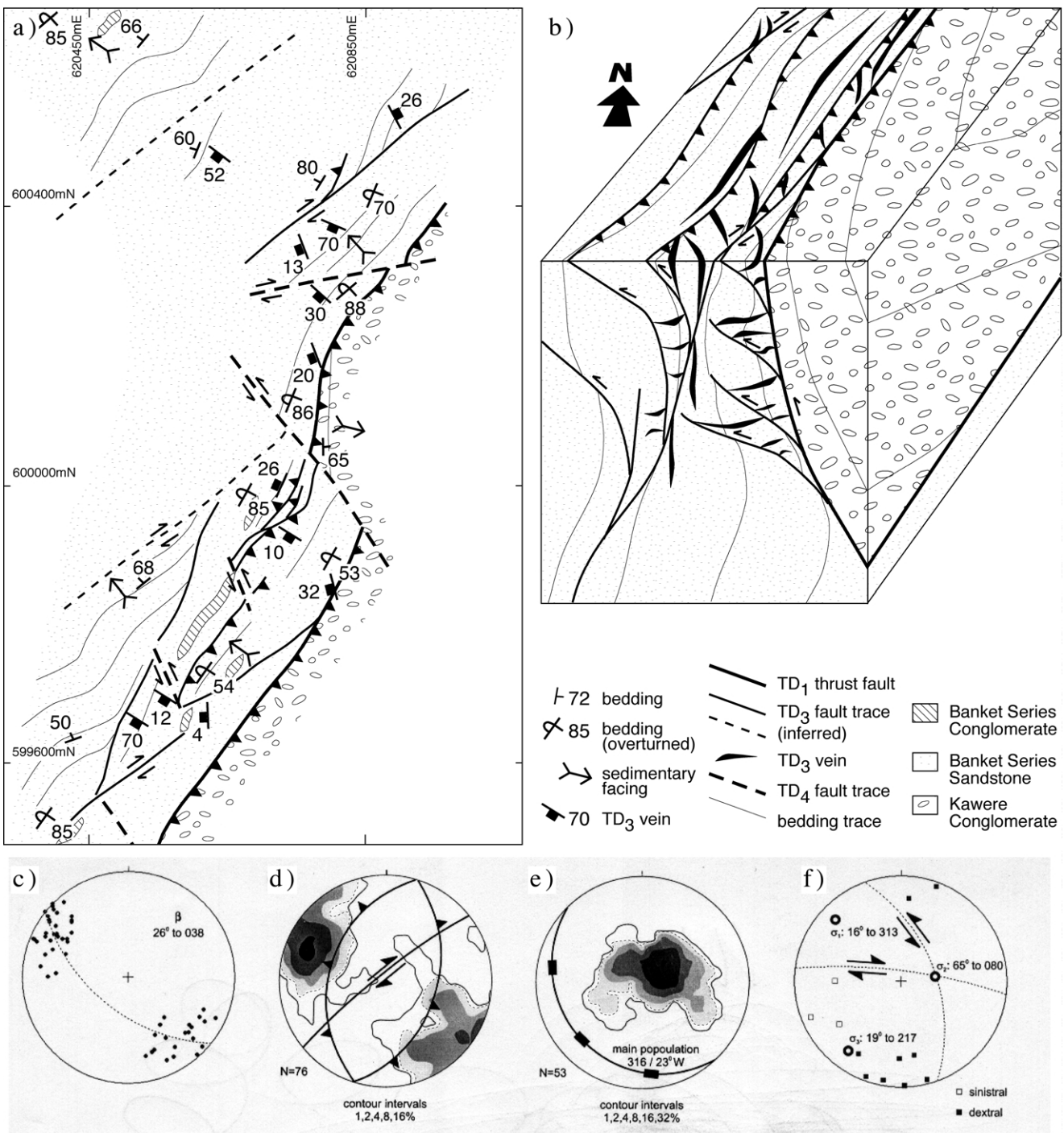


Fig. 6. Structural geology of Rex prospect. (a) The prospect is contained within Banket Series strata positioned on the NW limb of a TF1 anticline. Hinge of anticline is indicated by change in younging direction between Banket Series and Kawere strata, and is displaced along a NE striking $TD_1$ thrust. (b) Schematic block diagram indicating concentration of $TD_3$ thrusts and Au-bearing vein arrays within overturned strata positioned in immediate footwall of TD1 thrust. (c) Poles to bedding. The bulk of the data are derived from the NW limb of the $TF_1$ anticline, with SE dipping population largely representing strata overturned during $TD_3$. The shallowly NE plunging rotation axis is thus attributable mainly to $TF_3$. (d) Contoured poles to $TD_3$ faults, three main data populations exist: (i) moderately SE dipping, bedding sub-parallel thrusts, (ii) moderately NW dipping backthrusts, (iii) ENE striking sub-vertical faults with dextral wrench component. (e) Contoured poles to thrust-related $TD_3$ veins. Main SW dipping population lies sub-orthogonally to overturned strata within footwall of $TD_1$ thrust. (f) Poles to $TD_4$ faults. Conjugate fault array provides approximation of principal stress axes. (c)–(f) are lower hemisphere equal area projections.

down-dip extent, linking into major pre-existing structures that were favorably oriented for reactivation under ESE–WNW directed shortening. At Rex, for example, $TD_3$ structures display a close spatial association with a major SW-dipping $TD_1$ thrust fault, which bisects an antiformal $TF_1$ fold hinge (Fig. 6a and b). The largest populations of $TD_3$ faults involve near conjugate arrays of ESE and WNW dipping thrusts (Fig. 6d), which formed in response to brittle collapse and overturning within the footwall of the $TD_1$ thrust surface. A component of sub-vertically directed extension is also recorded in this structural position by high density, shallowly ESE-dipping, thrust-related $TD_3$ quartz veins arrays (Fig. 6e).

### 3.4. $TD_4$

Conjugate arrays of brittle strike-slip faults represent the final deformation event. $TD_4$ structures at Rex offset both the mineralization and the main $TD_1$ thrust and fold hinge (Fig. 6a). The two major fault strikes are: 325° (sinistral) and 080° (dextral). An acute angle of 65° between these conjugate sets is typical of upper crustal brittle fault zones (Ramsay and Huber, 1987) and consistent with a maximum compressive stress axis plunging shallowly NE (Fig. 6f).

## 4. Damang Mine geology and structure

There are two distinct styles of mineralization at Damang. The first is solely associated with the conglomerate horizons within the Banket Series. Here Au mineralization is developed as free gold in the matrix of the conglomerates. This style of mineralization is interpreted by Sestini (1973), Hirdes and Nunoo (1994) and this paper to be paleoplacer in origin and makes up approximately 20% of the total resource at Damang. The other style of Au mineralization is found in close spatial association with a series of flat lying to shallowly dipping quartz veins and quartz-filled faults and their accompanying alteration halos.

Mineralization at Damang Gold Mine is hosted by metamorphosed sediments that comprise all the units of the Tarkwaian Group (Table 1), with the exception of the Kawere Conglomerate. Dolerites, which intrude into the Tarkwaian Group, are also mineralized. At Damang all lithologies to the east of the Damang Fault in the mine sequence, including the dolerites, have been affected by mid-amphibolite facies metamorphism with temperature estimates based on garnet–biotite geothermometry of 550 °C (Pigois et al., 2003).

The currently defined economic deposit sits at the culmination of the gently NE plunging Damang Anticline (Fig. 2). Economic gold mineralization at Damang follows the general NE strike of the regional $TD_1$ structural grain. The orebody is approximately 3 km long and is open at depth in the northern end where it plunges gently towards 030°, parallel to the plunge of the Damang Anticline. It is also open at depth, to the limit of the current resource drilling, which extends to approximately 300 m below the original pre-mining surface. Mineralization is constrained on the west by the steeply east dipping Damang Fault.

The Damang Fault is interpreted to be a $TD_1$ thrust structure and at the current mining levels it has juxtaposed the folded Banket Series sandstones with west-dipping Huni Sandstone to the west (Fig. 7a and b). To the east the mineralization dies away shortly within the Huni Sandstone and 85% of the mineralization within the Damang Pit occurs in the units stratigraphically below the Huni Sandstone. The Tarkwa Phyllite seems to cap the bulk of the economic Au mineralization.

Where the Damang Fault and other similar faults have been located in drilling it is usually defined by a narrow zone (< 1 m thick) of intense foliation with narrow quartz tourmaline veins. SC fabrics and the abrupt change in metamorphic grade from greenschist facies in the west to amphibolite facies to the east of the fault support a dominantly reverse east over west sense of displacement. Because the maximum true thickness of the Huni Sandstone is unknown it is difficult to gauge the reverse displacement across the Damang Fault but a minimum throw is approximately 1 km based on stratigraphic reconstructions.

Other faults, which occur in the main part of the pit, have similar morphologies to the Damang Fault (e.g. The Huni, Juno and Railway Faults; Fig. 7) They strike northeast and dip subvertically or steeply to the west and east. Such faults commonly occur at the boundaries of lithological units, particularly the dolerites (Fig. 8a and b). Many of these faults have internal slickenlines and fibers, which enabled the sense of shear to be discerned. The fault striation data

Table 1
Stratigraphic subdivisions of the Tarkwaian group (after Brabham, 1998)

| | Subdivision | Thickness (m) | Lithologies |
|---|---|---|---|
| Tarkwaian | Huni Sandstone | >1300 | Fine-grained feldspathic sandstone and phyllite |
| | Tarkwa Phyllite | 100–350 | Plagioclase–tourmaline–chloritoid–chlorite–magnetite–carbonate–sericite argillite |
| | Banket Series | 150–600 | Lithic sandstone, quartz pebble conglomerate (Banket) and lithic polymict conglomerate |
| | Kawere Group | 250–700 | Lithic quartz sandstone, wacke, phyllite and polymict conglomerate |
| Birimian | | | Metasedimentary and metavolcanic rocks |

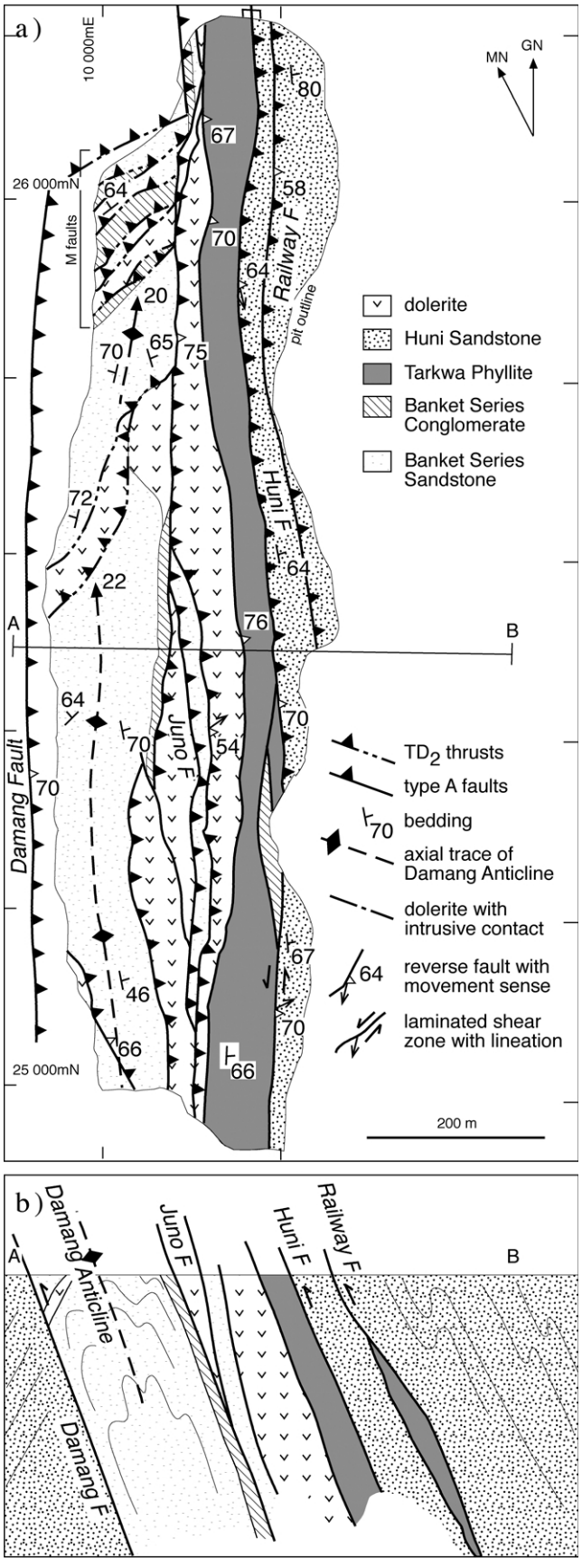


Fig. 7. Compilation of the mapped geology within the main portion of the Damang Gold Mine open pit at the 894 RL, which is approximately 100–145 m below the original pre-mining surface. The pit itself extends both to the north and south of this illustration although those areas were still dominantly within the oxide profile at the time of mapping. The trace of the Damang fault, which is shown outside the western wall of the pit, is only approximate and was located from the resource drilling data and by projection from higher levels in the pit. Location marks are shown in the local mine grid where north (GN) is at 032° to the east of magnetic north (MN).

enables a further subdivision of these structures into faults with sinistral strike-slip displacement and reverse faults (Fig. 9). Based on limited overprinting slickenlines it is interpreted that the reverse movement preceded the sinistral movement.

Immediately to the east of the Damang Fault lies the hinge of the Damang Anticline. Small-scale, tight to isoclinal folds with steep east dipping axial planes have been observed within the Tarkwa Phyllite, while more open, rounded folds occur in the Banket Series. The mine sequence dips steeply and is locally overturned on the western limb of the fold while the east limb dips uniformly at about 70° ESE (Fig. 10a). The $S_1$ cleavage associated with the Damang Anticline is only sporadically developed as a spaced, disjunctive, anastomosing to rough cleavage in the Banket sandstones. However $S_1$ is well developed within the Tarkwa Phyllite where it is manifest as a closely spaced, disjunctive, smooth cleavage that is near parallel to the $S_0$ fabric (Fig. 10b).

Towards the Northern end of the Damang Pit the Damang Fault steps to the east across a series of ENE–EW-trending steeply NNW dipping $TD_2$ faults locally known as the 'M' Faults (Fig. 7). Narrow zones of intense foliation and accompanying carbonate, muscovite quartz veins and sericite alteration mark these $TD_2$ faults. Although unmineralized, the 'M' faults are economically important as they have caused some thrust stacking of the Banket conglomerates in this area resulting in appreciably thickened zones of conglomerate hosted mineralization.

### 4.1. Gold mineralized veins

Mesothermal gold mineralization at Damang in associated with an array of flat-lying to shallowly dipping mineralized hydrothermal veins and faults locally termed QF (quartz flats; Fig. 11). QF veins are quartz dominant and display a variety of styles, which are summarized in Fig. 12 and detailed below. They are best developed within the silicified Banket Series and the dolerites. QF veins are developed moderately in the Tarkwa Phyllite and are restricted to coarse-grained silicified beds within the Huni Sandstone. This is to be expected during mixed-mode brittle failure where extension fractures tend to form in the most competent units while shear fractures form in less competent materials (Sibson, 2001). It is also an important

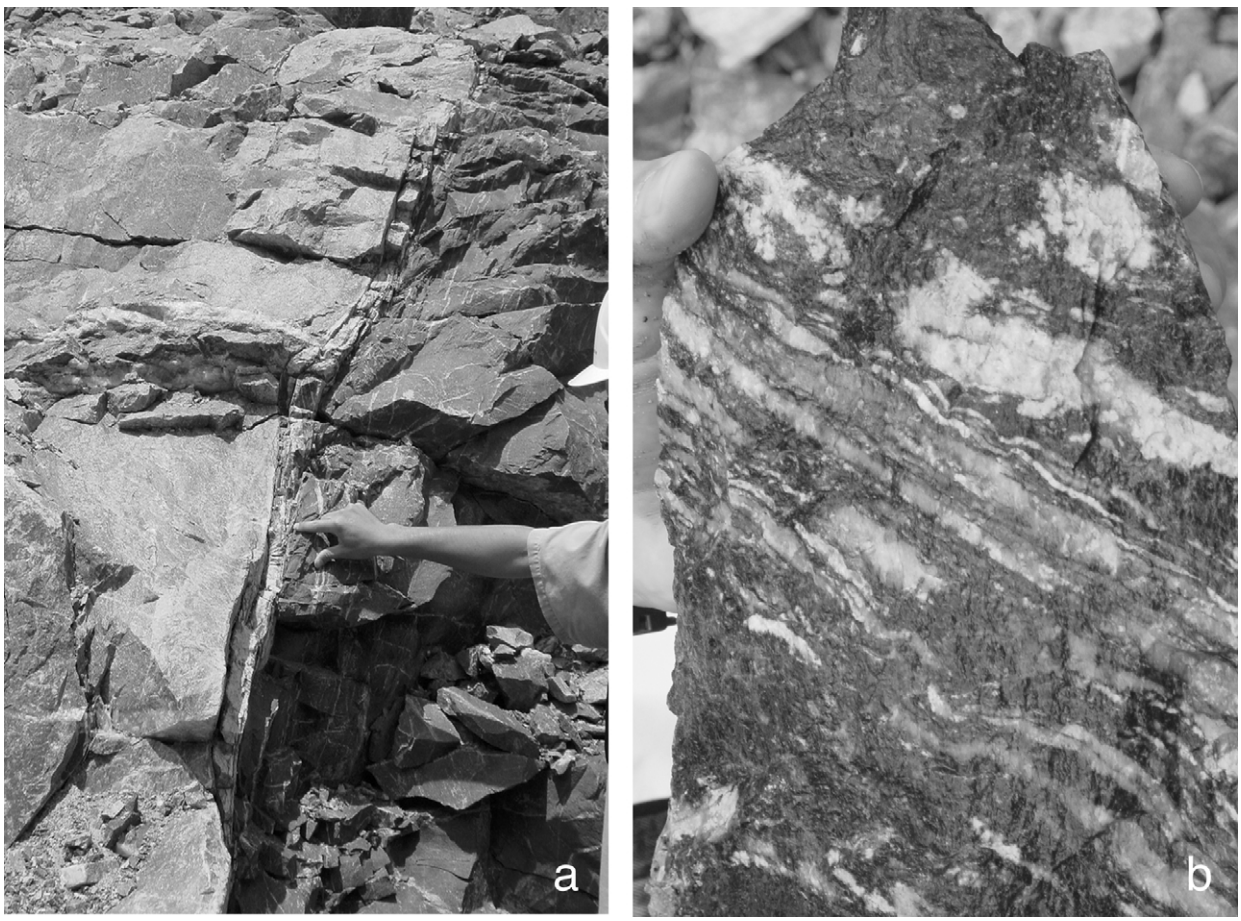


Fig. 8. (a) $TD_1$ fault at the contact between dolerite (to the right) and Banket sandstone. (b) Detail of a laminated $TD_1$ fault. Laminations comprise quartz, tourmaline minor carbonate and foliated wallrock.

point to note that all lithologies, including the dolerites, can have economic Au grades where they are cut by QF veins.

Narrow planar QF veins with high length/width ratios can be observed in the east walls of the pit where they are well developed within the Banket sandstone (Fig. 13a). Individual veins only several centimeters in width can be traced for over 50 m. Planar QF veins are mostly massive quartz veins with little or no internal textural variation, these veins are pure extensional veins with no shear offset.

Many QF veins possess a sigmoidal trace and form *en échelon* arrays (Fig. 13b). Sampling of both the veins and their extensive pyrite alteration halos show these veins are responsible for much of the hydrothermal gold mineralization present at Damang. These veins tend to form in weakly developed reverse-sense, shear zones that strike NE (between 025° and 045°) and dip shallowly to moderately both east and west.

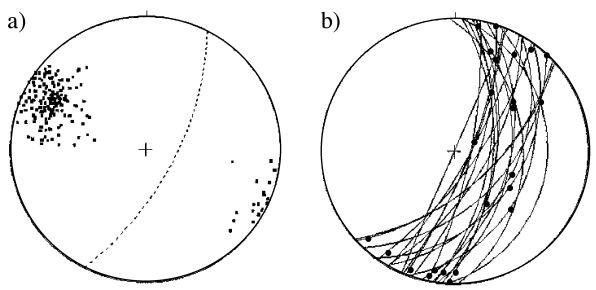


Fig. 9. Lower hemisphere equal area projections. (a) $TD_1$ faults, classification was made on orientation, the mean of the $TD_1$ data is shown as a great circle. (b) $TD_1$ faults where lineations were recorded. Limited overprinting relationships suggest the reverse movement preceded the strip-slip movement.

Another important style of QF veins is laminated fault-veins with multiple internal wall rock septa. They are commonly associated with narrow zones of weakly developed foliation and intense zones of sericite, quartz, carbonate and pyrite alteration. Fault-veins typically dip gently east although shallow west dipping examples have been also observed. The maximum displacement noted across a QF fault-vein was approximately 5 m and typically less than 1 m. QF fault-veins are typically accompanied by flat-lying extension veins that are usually unlaminated and of limited horizontal extent (Fig. 13c and d).

All QF veins are accompanied by a similar alteration assemblage that includes sericite + quartz + pyrite + chlorite ± gold ± pyrrhotite ± biotite ± calcite. These assemblages are typically wallrock buffered with the altered dolerite, Tarkwa Phyllite, Huni Sandstone and Banket Series sandstones all having slightly different alteration

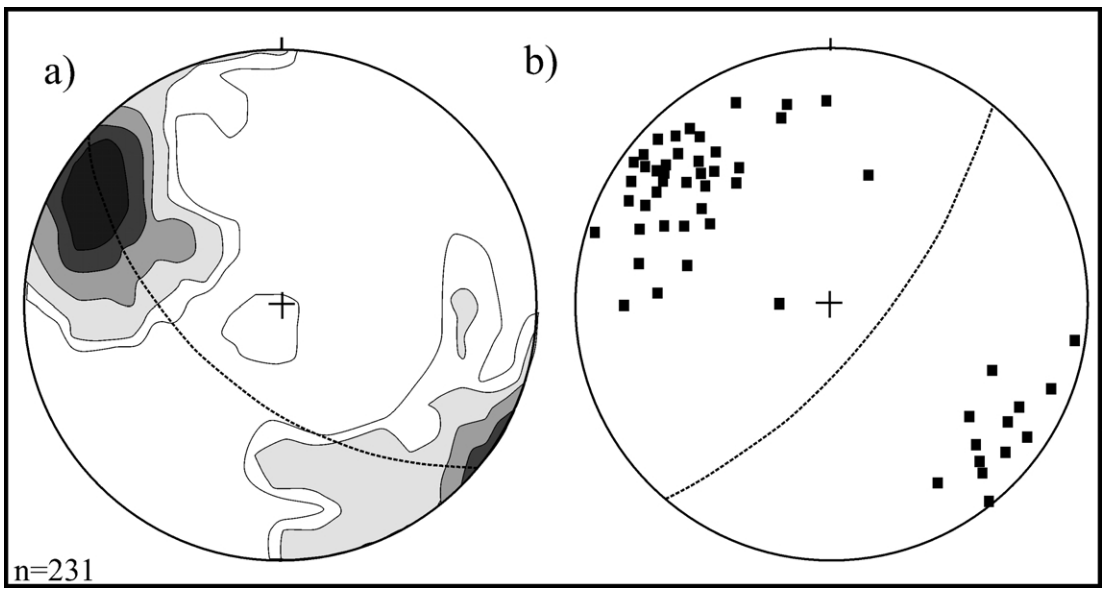


Fig. 10. Lower hemisphere equal area projections. (a) Contoured poles to bedding in all lithologies. The great circle represents best fit and the pole to great circle ($\beta$) indicates the calculated fold axis (contours at 2, 4, 8 and 16% of data where $n = 231$). (b) Poles to $S_1$ cleavage measured within the Damang pit, mean value is 040°/73SE.

assemblages. The presence of biotite, which is common in alteration selvedges around QF veins developed in dolerite and Tarkwa Phyllite, is indicative of temperatures in excess of 400 °C (Mikucki and Ridley, 1993).

### 4.2. Timing of the mineralization

The observed QF veins have a similar structural timing in that they cut the regional $S_1$ cleavage and $TD_1$ and $TD_2$ faults. Furthermore they appear to have developed within the same compressive stress field with $\sigma_3$ vertical, $\sigma_1$ oriented ESE–WNW and $\sigma_2$ oriented NNE–SSW. QF veins have mutually cross-cutting relationships where flat extension veins are cut by shallowly dipping laminated QF fault-veins, which are in turn cut by later extension veins. The alteration halos associated with the QF veins form a retrograde overprint on the peak metamorphic assemblage.

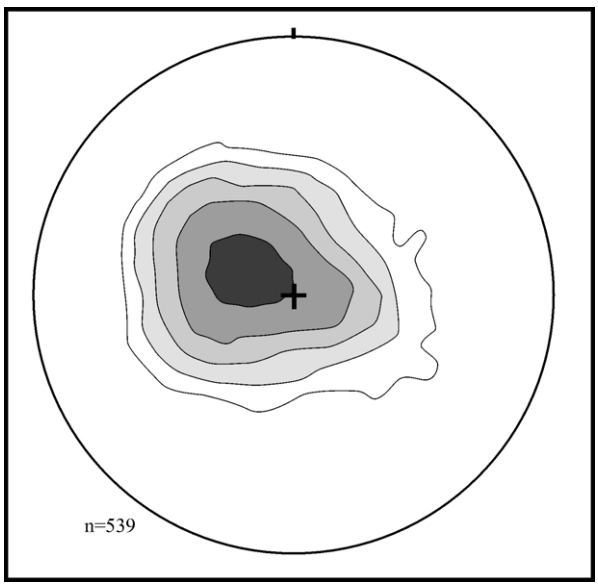


Fig. 11. Contoured hemisphere equal area projection. Poles to all QF veins and fault veins. (contours at 2, 4, 8 and 16% of data where $n = 539$).

There has been some minor reactivation of $TD_1$ faults during the $TD_3$ mineralization episode. These 030° striking faults, which commonly occur at lithological boundaries, were active during $TD_1$ as steep reverse faults and during $TD_2$ as sinistral strike-slip faults and have been to some extent reactivated during the $TD_3$ mineralizing event. Reactivation during $TD_3$ is evidenced by sporadic economic mineralization within the fault zones themselves and the rare presence of QF extension veins developed immediately adjacent to the faults (Fig. 12d). Limited fault lineation data indicates that the reactivation had a reverse sense of shear.

Based on their orientations, cross-cutting relationships with other structures and associated alteration halos QF veins appear to have developed late in the structural history of Damang ($TD_3$) and post the peak metamorphism. This is consistent with many Au vein and lode gold deposits classified as ‘Orogenic Lode Gold Deposits’ as described by Goldfarb et al. (2001).

### 4.3. Resource estimation and modeling

Initial observations of outcrop and measurements in oriented drill cores collected before the onset of mining in 1997 indicated unequivocally that quartz veins associated with gold mineralization were almost exclusively gently-dipping. Early resource estimates relied on cross-section interpretations of mineralization boundaries that conformed to the orientation of the QF veins (Fig. 14a), except where

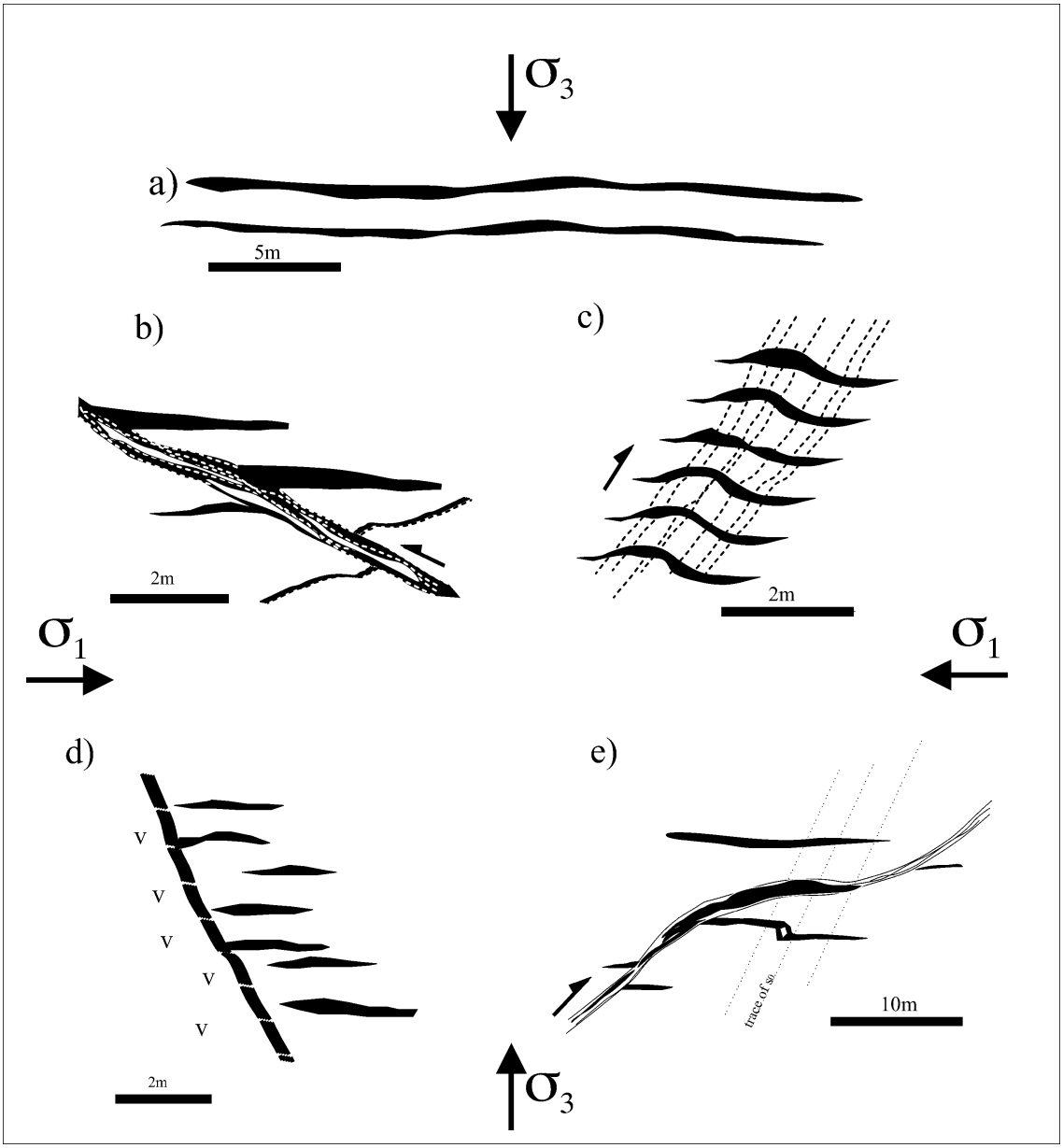


Fig. 12. Various mineralized QF veins from E–W mining exposures at Damang. Also indicated is the inferred stress direction at the time of mineralization. (a) Isolated extension veins. (b) Laminated thrust with accompanying extension veins. (c) En échelon extension veins forming in the hanging wall of a reactivated $TD_1$ fault. (e) Thrust with ramp and flat geometry (note the substantial thickening of internal quartz veins in flat section of thrust, which acts as a dilational jog).

gold was obviously hosted by Banket conglomerate in stratabound paleoplacer lodes.

At the commencement of mining in 1997, close-spaced (6 m × 8 m) grade-control drill sampling became available. It rapidly became obvious that the orientations of some ore shoots were quite different to the interpretations based on the initial drilling and interpreted to be flat or gently dipping. On the sub-vertical, attenuated western limb of the Damang Anticline ore lenses predominantly dipped to the west (Fig. 14b). On the eastern limb of the anticline ore zones dipped to both the west and the east, with east dips dominant in most of the mines. The strike of individual ore shoots was also variable from about 015° through to 040°.

Early resource models computed using geostatistical techniques—multiple indicator kriging (MIK)—that relied on interpretations of sub-horizontal ore zones based on the known flat vein geometry underestimated ore tonnages by approximately 40%.

Gold deposits where the mineralization is controlled by complex 3D vein and fault networks represent one of the most difficult types of gold mineralization in which to reliably estimate the economic gold resources. Damang is a good example of a deposit in which the complexity of structural controls precludes resource estimation using techniques that require manual interpretation of ore limits, e.g. polygonal or wire-framing approaches. Early resource

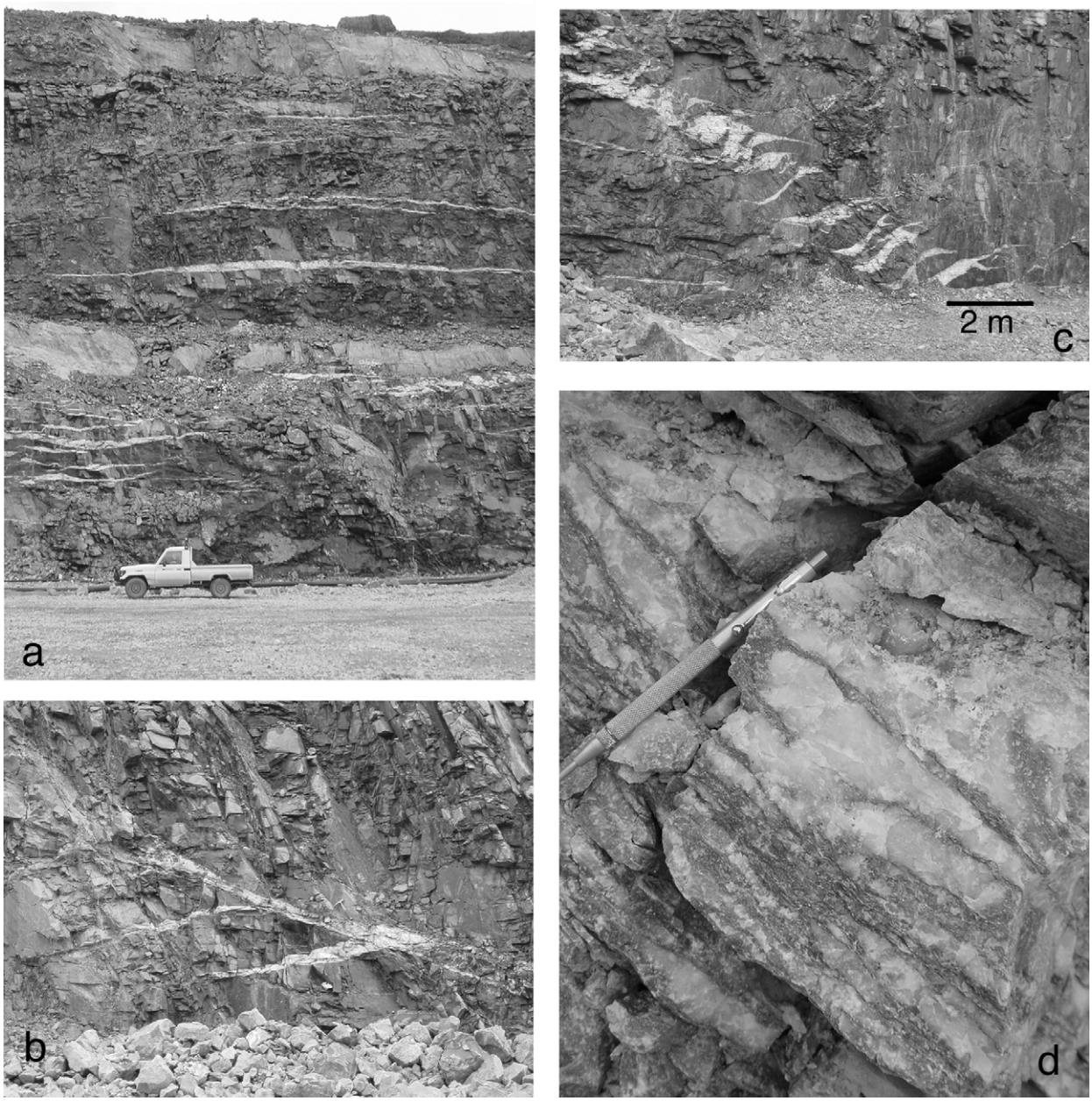


Fig. 13. (a) Detail of individual QF veins in the eastern wall of the Damang Pit, note the planar nature of the veins and the height/width ratio. (b) Moderately west-dipping, reverse sense brittle–ductile shear zone. (c) Photograph looking north in northern Damang pit showing a shallowly east dipping thrust fault and accompanying gently dipping extensional veins. (d) Detail of laminations within QF quartz filled thrust in central portion of Damang pit. Laminations comprise wallrock inclusions, fine-grained pyrite and rate tourmaline and chlorite.

estimates were compromised by the imposition of a misconception of the structural controls on mineralization. From the commencement of mining geostatistical techniques have been used to make reliable ore/waste decisions in grade control. Resource modeling is also undertaken using geostatistical methods (MIK) with little geological control imposed.

## 5. Discussion

The Damang Gold Deposit is unique amongst the documented deposits of Ghana in that it is the single place where two distinct styles and timings of Au mineralization are clearly present. The first style of mineralization is that associated with the conglomerate horizons within the Banket Series. Here mineralization is completely stratabound and gold occurs as free gold associated with both fine-grained detrital and authigenic hematite and magnetite in the matrix of the conglomerates. Economic gold grades occur in the conglomerate in the absence of QF veins and alteration. However, grades can be significantly improved where QF veins and alteration cut the conglomerates. The Banket Series conglomerates represent the earliest gold

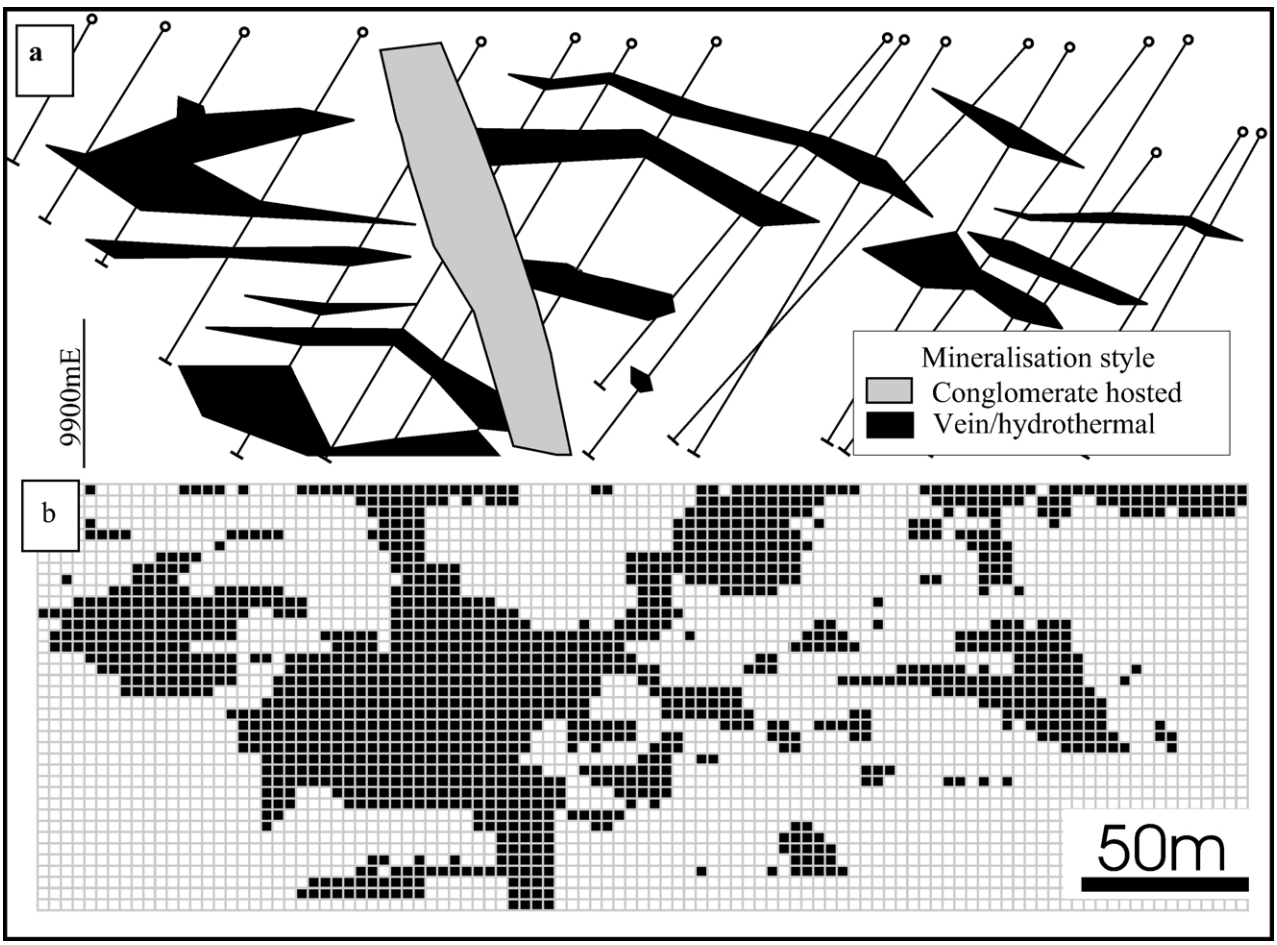


Fig. 14. Two versions of the same cross-section at 25370N (local grid) looking north showing the modeled 0.6 g/t cut-off. In (a) the ore body geometry was modeled to parallel the observed flat geometry of the QF veins. The Banket conglomerate hosted mineralization is also shown and this was modeled separately based on the dip of the conglomerate. (b) Indicator kriging model using no geological constraints at the same cut-off grades, but with the additional data of the detailed grade control drilling (not shown 6 × 8 m pattern). Note the true orientations of the ore bodies are steep to moderately dipping parallel to the stacked arrays of veins rather than parallel to the flat veins themselves.

mineralization known in the area and are interpreted to be paleoplacer gold deposits that have been slightly modified by subsequent metamorphism and deformation (Sestini, 1973; Hirdes and Nunoo, 1994). The source of the paleoplacer gold remains unclear (Pigois et al., 2003).

Regionally the major folds within the Damang area strike to the northeast indicating approximately NW–SE shortening. The present location of the Damang gold deposit occurs where the Damang Fault cuts up through the stratigraphy and thrusts the Banket Series over itself and the stratigraphically younger Huni Sandstone. Although small-scale folds are present throughout the mine sequence strong foliation development and tight to isoclinal folding is restricted to the Tarkwa Phyllite. This suggests it was the mechanically weakest unit present within the sequence and underwent the highest ductile strains during early deformation and metamorphism.

The $TD_1$ faults have developed early in the deformation history; yet have been reactivated during $TD_2$ (sinistral reactivation) and $TD_3$ (reverse reactivation). There are two possible origins for the $TD_1$ faults. In the first scenario, they represent break-through thrusts accommodating progressive fold tightening during the latter stages of the $TD_1$ event. A consequence of this model is that the structures may not have existed prior to the main folding event and thus have limited depth extent. The second scenario involves reactivation of pre-Tarkwaian extensional structures during the onset of $TD_1$ shortening. In this case, favorably oriented deep-seated structures had the potential to nucleate folds within the Tarkwaian cover sequence at the onset of NW–SE compression. Thus $TF_1$ folds may partly involve a wrench origin, with nucleation and amplification of anticlinal closures above major NNE fault zones; hence, the spatial association of 'break-through' thrusts and $TF_1$ anticlines. Although this argument seems esoteric, the question as to whether the thrusts are shallow- or deep-seated has significant implications for the plumbing system during the main mineralizing phase, particularly in terms of tapping fertile Birimian basement rocks at depth. If the plumbing systems were deep-seated, then favorable lithologies within the Birimian volcanics could also be prospective.

N–S shortening during $TD_2$ led to the development of the new ENE oriented thrusts and sinistral strike-slip reactivation of $TD_1$ faults. Structures formed during $TD_2$ are not mineralized and therefore were not active during the later hydrothermal event that brought in the gold. The 'M' faults in the northern part of the Damang pits do have some bearing on the economics of the mine as they cause thrust bound repetitions of the Banket conglomerate.

The bulk of the gold mineralization at Damang is associated with arrays of flat-lying to gently-dipping quartz veins and small displacement thrust faults. These features have combined to result in a fracture array network in which orebody geometry is not parallel to individual flat-lying or gently dipping QF structures but rather parallel to the enveloping surface of arrays of QF structures.

### 5.1. Interpretation of the mineralized vein system

The presence of Au mineralized, flat-lying to gently dipping extension veins indicates a compressive stress regime where $\sigma_3$ is subvertical and requires that the fluid pressures were, at least locally, supralithostatic during the mineralization event. The extensional and extensional shear nature of the veins combined with the low displacements on $TD_3$ thrusts active at the time of mineralization further implies low values of differential stress (Etheridge, 1983). It is also possible that the strongly foliated Tarkwa Phyllite acted as an effective cap to fluid pressures during the mineralization episode allowing the fluid pressure to build up underneath it. This interpretation is supported by the fact that the bulk of the mineralization at Damang is found stratigraphically below the Tarkwa Phyllite.

The generation of lithostatic and supralithostatic fluid pressures beneath a caprock can only be maintained in the absence of through-going cohesionless faults that are well oriented for reactivation in the prevailing stress field (Sibson, 2001). The angle between a sub-horizontal $\sigma_1$ oriented at 120° and the through-going $TD_1$ faults is approximately 60–70°. It would appear from the presence of rare mineralized laminations within the $TD_1$ faults that they have been episodically reactivated during the mineralization event. The fact that strongly misoriented faults $TD_1$ do reactivate during the $TD_3$ is further evidence of lithostatic or supralithostatic fluid pressures and perhaps fault valve mechanisms (e.g. Sibson et al., 1988). This interpretation is supported by $TD_3$ laminated fault veins and the mutually cross-cutting nature of the QF veins indicating multiple slip increments accompanied by episodic fluid discharge, both diagnostic of cyclical fault-valve action (Sibson, 1996; Nguyen et al., 1998; Cox et al., 2001). Fault valve behavior has been documented from several well-known gold districts including the Revenge gold mine, Kambalda, where optimally oriented shear zones were reactivated by fault valve action (Nguyen et al., 1998). The majority of other examples for fault valve behavior come from systems where the major faults are severely

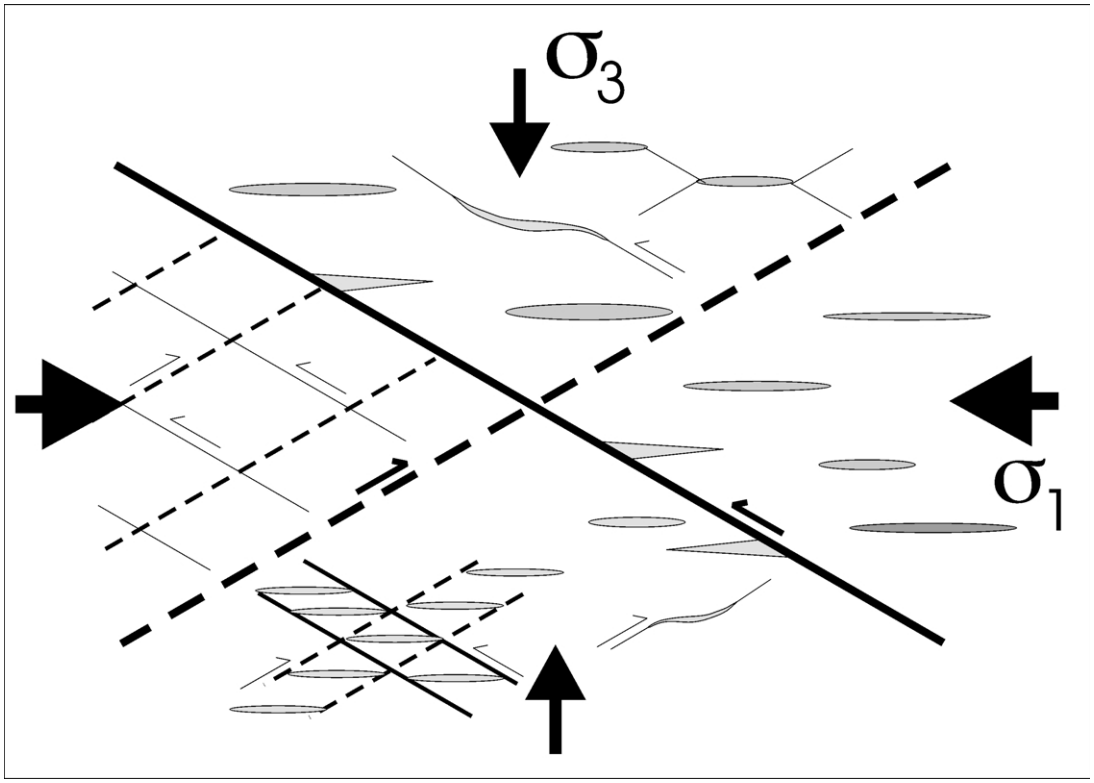


Fig. 15. Possible stress controlled components of structural permeability developed in a fault–fracture mesh in relation to a compressional stress field in the orientations interpreted for Damang during the hydrothermal event (adapted from Sibson (2001)).

misoriented, e.g. the Sigma Mine, Abitibi (Boullier and Robert, 1992) and the Central Victorian goldfields of Bendigo and Ballarat (Cox, 1995; Cox et al., 1991).

The formation of a series of thrust faults and linked extension veins is referred to in the literature as a 'Fault–Fracture Mesh' (Hill, 1977; Sibson, 1996) and the development of QF veins and faults at Damang is remarkably similar to that postulated for fault–fracture meshes by Sibson (1996, 2001) (Fig. 15). A further implication of the fault–fracture mesh model is that the greatest direction of structurally enhanced permeability for fluids is the $\sigma_2$ direction (Cox et al., 2001; Sibson, 2001), which in the case of Damang lies approximately NE parallel to the regional $TD_1$ fold axis. Similar combinations of reverse faults, extensional veins and fold hingelines are also thought to support channeled fluid flow during the mineralization at Bendigo (Cox et al., 1991).

The focusing of ascending hot hydrothermal fluids in antiformal closures has been modeled theoretically by Matthai (1994), who showed that it is an effective method of concentrating hydrothermal fluid. At Damang hydrothermal fluids may have reacted with the down-faulted Banket Series conglomerates on the western side of the Damang Fault and/or Banket conglomerates deeper down the eastern limb of the fold, and these fluids may have sourced gold from the paleoplacer gold accumulations in the conglomerates (Fig. 16). The paleoplacer Au rich conglomerates would have provided an excellent source rock with high (ppm level) gold values. These fluids were continually focused into the anticline and trapped under the Tarkwa Phyllite, which is believed to act as an effective cap, resulting in elevated fluid pressures and the formation of the fault–fracture mesh.

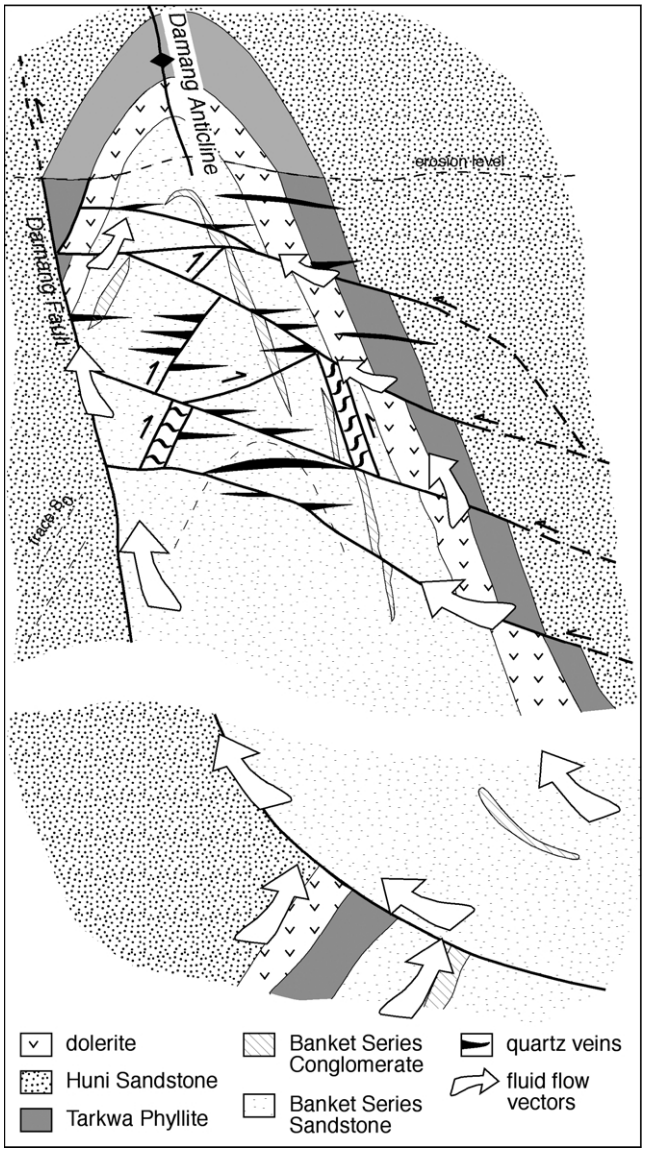


Fig. 16. Schematic cross-section illustrating the model for the development of the fault–fracture network and associated hydrothermal mineralization at Damang. It is suggested that hot ascending hydrothermal fluids from an unknown source are initially focused into the Damang Anticline. The Damang Fault is shown shallowing at depth consistent with it being a reactivated extensional structure although this is not central to the model. The late hydrothermal fluids potentially derive gold from the overthrust Banket conglomerates containing the paleoplacer mineralization. These fluids are continually focused into the anticline and trapped under the Tarkwa Phyllite, which is believed to act as an effective cap, resulting in elevated fluid pressures and the formation of the fault-fracture network shown.

## 6. Conclusions

The majority of the gold at the Damang Gold mine is the product of post metamorphic, low differential stress, high fluid pressure conditions allowing the formation and activation of a low-displacement, fault–fracture mesh in a compressional stress regime. Hydrothermal mineralization is associated with pyrite and pyrrhotite in quartz carbonate sericite alteration halo about flat lying to gently dipping quartz veins and low-displacement reverse faults. This mineralization overprints an earlier style of paleoplacer gold that is restricted to the conglomerates of the Banket Series.

The exposed mineralized vein geometries in low-displacement fault–fracture meshes are excellent examples of vein formation and mineralization under conditions of high fluid-pressure and low differential-stress late in the tectonic cycle. It is interpreted that the source of the gold for the hydrothermal event may have been the early Banket conglomerate mineralization.

## Acknowledgements

Vic King and Bruce Stainforth of Ghana Goldfields are thanked for permission to publish this work. Discussions with Paul Woolrich, John Pigois, Rod Marston, Gyedu Nketia, Felix Dong and Sam Anie have assisted in our understanding of the geology at Damang. Rick Sibson and Andrew Allibone are thanked for detailed, insightful

reviews, which have greatly improved this work. Stereonets were plotted using Rod Holcombe's excellent Georient program.

## References


Allibone, A., Teasdale, J., Cameron, G., Etheridge, M., Uttley, P., Soboh, A., Appiah-Kubi, J., Adanu, A., Arthur, R., Mamphey, J., Odoom, B., Zuta, J., Tsikata, A., Patayc, F., Famiyeh, S., Lamb, E., 2002a. Timing and structural controls on gold mineralization at the Bogoso gold mine, Ghana, West Africa. Economic Geology 97, 949–969.

Allibone, A., McCuaig, C.T., Harris, D., Etheridge M., Munroe, S., Byrne, D., Amanor, J., Gyapong, W., 2002. Structural controls on gold mineralization at the Ashanti Gold Deposit, Obuasi, Ghana. In: Goldfarb, R.J., Neilson, R.L. (Eds.), Integrated Methods for Discovery: Global Exploration in the 21st Century. Society of Economic Geologists Special Publication 9, pp. 65–93.

Appiah, H., 1991. Geology and mine exploration trends of the Prestea goldfields, Ghana. Journal of African Earth Sciences 13, 235–241.

Blenkinsop, T., Schmidt, M., Kumi, R., Sangmoor, S., 1994. Structural geology of the Ashanti Goldmine. Geologisches Jahrbuch D100, 131–153.

Boullier, A., Robert, F., 1992. Paleoseismic events recorded in Archaean gold-quartz vein networks, Val d'Or, Abitibi, Quebec, Canada. Journal of Structural Geology 20, 161–179.

Brabham, G., 1998. The regional geological setting and nature of the Damang stockwork gold deposit—a new type of gold deposit in Ghana. Masters Thesis. University of Western Australia, W.A., Perth.

Cox, S.F., 1995. Faulting processes at high fluid pressures: an example of fault-valve behaviour from the Wattle Gully Fault Victoria, Australia. Journal of Geophysical Research 100, 841–859.

Cox, S.F., Wall, V.J., Etheridge, M.A., Potter, T.F., 1991. Deformational and metamorphic processes in the formation of mesothermal vein-hosted gold deposits; examples from the Lachlan fold belt in central Victoria, Australia. Ore Geology Reviews 6, 391–423.

Cox, S.F., Knackstedt, M.A., Braun, J., 2001. Principles of structural control on permeability and fluid flow in hydrothermal systems. Society of Economic Geologists Reviews 14, 1–24.

Davis, D.W., Hirdes, W., Schaltegger, U., Nunoo, E., 1994. U–Pb age constraints on deposition and provenance of Birimian and gold-bearing Tarkwaian sediments in Ghana, West Africa. Precambrian Research 67, 89–107.

Eisenlohr, B.N., Hirdes, W., 1992. The structural development of the early Proterozoic Birimian and Tarkwaian rocks of southwest Ghana, West Africa. Journal of African Earth Sciences 3, 313–325.

Etheridge, M.A., 1983. Differential stress magnitudes during regional deformation and metamorphism: upper bound imposed by tensile fracturing. Geology 11, 231–234.

Goldfarb, R.J., Groves, D.I., Gardoll, S., 2001. Orogenic gold and geologic time; a global synthesis. Ore Geology Reviews 18, 1–75.

Hill, D.P., 1977. A model for earthquake swarms. Journal of Geophysical Research 82, 1347–1352.

Hirdes, W., Nunoo, B., 1994. The Proterozoic paleoplacers at Tarkwa gold mine, SW Ghana; sedimentology, mineralogy, and precise age dating of the Main Reef and West Reef, and bearing of the investigations on source area aspects. Geologisches Jahrbuch D100, 247–311.

Hirdes, W., Davis, D.W., Eisenlohr, B.N., 1992. Reassessment of Proterozoic granitoid ages in Ghana on the basis of U, Pb, zircon and monazite dating. Precambrian Research 56, 89–96.

Hirst, T., 1938. The geology of the Tarkwa Goldfield and adjacent country. Gold Coast Geological Survey Bulletin 10.

John, T., Klemd, R., Hirdes, W., 1999. The metamorphic evolution of the Paleoproterozoic Birimian volcanic Ashanti belt Ghana, West Africa. Precambrian Research 98, 11–30.

Junner, N.R., Hirst, T., Service, H., 1942. The Tarkwa Goldfield. Gold Coast Geological Survey Memoir 6.

Leube, A., Hirdes, W., Mauer, R., Kessie, G.O., 1990. The early Proterozoic Birimian Supergroup of Ghana and some aspects of its associated gold mineralisation. Precambrian Research 46, 139–165.

Marston, R.J., Woolrich, P., Kwesie, J., 1992. Closely associated stockwork and palaeoplacer gold mineralisation in the early Proterozoic Tarkwaian System of Abosso, SW Ghana. In: Peters, J.W., Kesse, G.O., Acquah, P.C. (Eds.), Regional Trends in African Geology. Proceedings of the 9th International Geological Conference, Accra, 1992, pp. 243–271.

Matthai, S.K., 1994. Genesis of intrusion related hydrothermal gold deposits. Doctoral Thesis Australian National University, Canberra, A.C.T.

Mikucki, M., Ridley, R.J., 1993. The hydrothermal fluid of Archaean lode-gold deposits at different metamorphic grades; compositional constraints from ore and wallrock alteration assemblages. Mineralium Deposita 28, 469–481.

Nguyen, P.T., Cox, S.F., Harris, L.B., Powell, C.McA., 1998. Fault valve behaviour in optimally oriented shear zones: an example at the Revenge gold mine, Kambalda, Western Australia. Journal of Structural Geology 20, 1625–1640.

Oberthur, T., Vetter, U., Davis, D.W., Gyapong, W.A., 1998. Age constraints on gold mineralisation and Paleoproterozoic crustal evolution in the Ashanti belt of Southern Ghana. Precambrian Research 89, 129–143.

Pigois, J.P., Groves, D.I., Fletcher, N., McNaughton, N., Snee L.W., 2003. Constraints on the age of Birimian gold mineralisation and source of the Tarkwaian paleoplacers in Ghana: SHRIMP II U–Pb ages of detrital zircons and hydrothermal xenotime from the Tarkwa Damang gold district. Mineralium Deposita, 38, 695–714.

Ramsay, J.G., Huber, M., 1987. The Techniques of Modern Structural Geology. Volume 2: Folds and Fractures. Academic Press, London.

Sestini, G., 1973. Sedimentology of a palaeoplacer: the gold-bearing Tarkwaian of Ghana. In: Amstutz, G.C., Bernard, J.A. (Eds.), Ores in Sediments, pp. 275–306.

Sibson, R.H., 1996. Structural permeability of fluid-driven fault-fracture meshes. Journal of Structural Geology 18, 1031–1042.

Sibson, R.H., 2001. Seimogenic framework for hydrothermal transport and ore deposition. Society of Economic Geologists Reviews 14, 25–50.

Sibson, R.H., Robert, F., Poulsen, K.H., 1988. High-angle reverse faults, fluid pressure cycling and mesothermal gold deposits. Geology 16, 551–555.

Strogen, P., 1988. The sedimentology, stratigraphy and structure of the Tarkwaian, Western Region, and its relevance to gold exploration and development. In: Kesse, G.O. (Ed.), Proceedings of the International Conference on the Geology of Ghana with Special Emphasis on Gold, V3. Geological Society of Ghana, Accra, 1988, pp. Hl–H31.

Whitelaw, O.A.L., 1929. The geology and mining features of the Tarkwa–Abosso goldfield. Gold Coast Geological Society Memoir 1.